# Surface tension and fingering of miscible interfaces

Mohammed Abid, Jian-Bang Liu and Paul D. Ronney
Department of Aerospace and Mechanical Engineering
University of Southern California, Los Angeles CA 90089-1453 USA

**Abstract**

Experiments on miscible, buoyantly unstable reaction-diffusion fronts and non-reacting displacement fronts in Hele-Shaw cells show a fingering-type instability whose wavelengths ($\lambda^*$) are consistent with an interfacial tension ($\Sigma$) at the front caused by the change in chemical composition, even though the solutions are miscible in all proportions. In conjunction with the Saffman-Taylor model, the relation $\Sigma \approx K/\tau$, where $\tau$ is the interface thickness and $K \approx 4 \pm 2 \times 10^{-6}$ dyne, enables prediction of our measured values of $\lambda^*$ as well as results from prior experiments on miscible interfaces. These results indicate that even for miscible fluids, surface tension is generally a more significant factor than diffusion in interfacial stability and flow characteristics.

PACS classifications: 05.70.Np, 47.20.-k, 47.20.Ma, 68.10.C

**Address correspondence to:**

Paul Ronney
Department of Aerospace and Mechanical Engineering
University of Southern California
OHE 430J
Los Angeles, CA 90089-1453
(213) 740-0490
(213) 740-8071 (fax)
ronney@usc.edu

Submitted to *Physical Review Letters*, November, 1999

## Introduction

A Hele-Shaw cell is perhaps the simplest system in which multi-dimensional convection is present and is used extensively as a model hydrodynamic system [1]. Buoyant convection and viscosity contrast cause instability of displacement fronts between non-reacting immiscible [1] and miscible [1, 2] fluids as well as propagating reaction-diffusion fronts [3, 4, 5] in Hele-Shaw cells. A key instability characteristic is the wavelength ($\lambda^*$) of the first fingers observed on an initially flat interface, given by $2\pi/k^*$, where $k^*$ is the wavenumber corresponding to the maximum growth rate ($\sigma^*$) of infinitesimal interfacial disturbances. To obtain a finite value of $k^*$, a mechanism is needed to suppress disturbances of large k. This mechanism is thought to be surface tension for immiscible interfaces [1] and diffusion for miscible nonreacting [1, 2] or reacting [3, 4, 5] interfaces.

Saffman and Taylor [6] derived a $\sigma$-k relation for a non-reacting immiscible interface between a displaced fluid (subscript "1") and a displacing fluid (subscript "2") in a Hele-Shaw cell:

$$\sigma = \left[\frac{\mu_1 - \mu_2}{\mu_1 + \mu_2} U + \left(\frac{\rho_1 - \rho_2}{\mu_1 + \mu_2}\right)\frac{g w^2 \cos(\theta)}{12}\right] k - \frac{\Sigma w^2}{12(\mu_1 + \mu_2)} k^3 \qquad (1)$$

where $\mu$ is the dynamic viscosity, g the gravitational acceleration, $\rho$ the density, $\theta$ the angle of the cell from vertical, U the speed at which the displacing fluid is forced into the displaced fluid, $\Sigma$ the surface tension and w the cell gap. For the conditions studied in this work the temperature and concentration changes across the fronts are far too small to cause the viscosity contrast term to be competitive with the buoyancy term; in this case Eq. (1) predicts

$$\lambda^* = 2\pi\sqrt{\frac{3\Sigma}{\rho g \delta \cos(\theta)}};\quad \sigma^* = \frac{w^2}{36\mu}\sqrt{\frac{[\rho g \delta \cos(\theta)]^3}{3\Sigma}} \qquad (2),$$

where $\delta \equiv (\rho_1 - \rho_2)/\rho_1$ is the dimensionless density contrast.

For miscible fronts it is thought that surface tension does not plays a role and instead diffusion suppresses high-k disturbances [1]. For reaction-diffusion fronts the σ-k relation with $\Sigma = 0$ and $\mu_1 - \mu_2 = 0$ [4] is the same as Eq. 1 with U replaced by the front propagation speed (s) and the surface tension term replaced by $k^2D$, where D is the reactant diffusivity. This leads to

$$\lambda^* = C_1 \frac{\mu D}{\rho g \delta \cos(\theta) w^2}; \quad \sigma^* = \frac{C_2}{D}\left(\frac{\rho g \delta \cos(\theta) w^2}{\mu}\right)^2 \qquad (3),$$

where $C_1 = 96\pi$ and $C_2 = 1/2304$. For reaction-diffusion fronts the interface thickness ($\tau$) = D/s [3, 4] is time-independent. For non-reacting displacement fronts $\tau$ increases with time, but a σ-k relation has been derived assuming initially $\tau = 0$ [1, 7]. This relation leads to Eq. (3) again but with $C_1 = 96\pi/(\sqrt{5}-2)$ and $C_2 = 0.000391$.

In this Letter we show that even for miscible fronts, a weak effective surface tension exists that is generally a more significant mechanism in wavelength selection (via Eq. 2) than diffusional effects (Eq. 3) because it results in a much smaller $\sigma^*$ than would occur were $\Sigma = 0$. While prior experiments have noted evidence of surface tension at miscible interfaces [8, 9, 10], a difficulty in quantifying this evidence exists because for displacement fronts $\tau$ increases over time due to diffusion. In contrast, for reaction-diffusion fronts $\tau$ is constant, thus a constant $\Sigma$ may exist. We will show that $\Sigma$ and thus instability characteristics can be predicted for both types of interfaces using a single simple model.

**Experimental apparatus and procedures**

Experiments were conducted in Hele-Shaw cells made of transparent Lexan. The cell dimensions were 200 mm x 200 mm x w, with 0.18 mm < w < 3 mm. The estimated Reynolds numbers $\approx (\sigma^*/k^*)w/\nu$ of the resulting flows in the initial stage of instability is less than 4 for all cases studied, thus laminar Pouseille flow prevails.

For reaction-diffusion fronts, the hydrosulfite-iodate autocatalytic system [11] was used, which has the overall reaction $S_2O_4^{2-} + IO_3^- + H_2O \rightarrow 2SO_4^{2-} + I^- + 2\,H^+$. A typical composition

was $[S_2O_4^{2-}] = [IO^-_3] = 0.015$ M with NaOH added to obtain pH = 12, for which s = 0.020 cm/s. Values of s between 0.0015 and 0.042 cm/s were obtained by varying the chemical composition. The fronts were visualized using the natural color change or enhanced using pH indicators. Due to the slight temperature rise and composition changes across the front (discussed later), the products are less dense than the reactants, thus upward-propagating fronts are buoyantly unstable. The experiments were conducted by initiating fronts at the top of the cell and, after a flat downward propagating front developed, sealing the cell and inverting it.

For non-reacting displacement fronts, the experiments were conducted in a manner similar to Wooding [2]. The lower part of the cell was filled with the more-dense fluid, a horizontal barrier strip was inserted, and the upper part was filled with the less-dense fluid. The barrier was pulled horizontally out of the cell to start the experiment.

Values of $\lambda^*$ were determined from images of the interface in the early stage of fingering, either by counting the fingers over a known width of the cell as in [2, 5], or determined from the peaks of spatial Fourier transforms of the fronts. There was no statistically significant difference between the two methods. The typical standard deviation of $\lambda^*$ in one experiment was $0.2\lambda^*$, which exceeds the uncertainty in the measurement of $\lambda^*$ itself. Measured standard deviations will be shown below for displacement fronts.

For reaction-diffusion fronts, the (temporary) temperature-induced fractional density change $\delta_T$ (typically $6 \times 10^{-4}$) was determined by calculating the thermodynamic temperature rise and applying the thermal expansion coefficient of water. This rise was checked experimentally using a thermocouple immersed in the solution; the difference was less than 10% in all cases tested. The (permanent) concentration-induced fractional density change $\delta_C$ was measured using a home-made dilatometer. $\delta_T/\delta_C$ varied from about 20 for $[IO_3^-] << [S_2O_4^{2-}]$ to about 4 for $[IO_3^-] \geq [S_2O_4^{2-}]$. Except as noted, all calculations for reaction-diffusion fronts employ $\delta = \delta_T + \delta_C$.

**Results - reaction diffusion fronts**

Shortly after inversion the fronts began to exhibit fingers, a typical image of which is shown in Fig. 1 (upper). Figure 2 (left) shows $\lambda^*$ for varying Peclet number $Pe \equiv Uw/D$, where $U = \sigma^*/k^*$ is the phase velocity of the most amplified linear mode according to Eq. 2 ($\sigma^*/k^*$ from Eq. 3 yields the same U and thus Pe except for a factor of 3/4) and $D \approx 1.4 \times 10^{-5}$ cm$^2$/s is the mass diffusivity of $IO_3^-$ [12]. With this definition $Pe = (1/36)(\rho g \delta \cos(\theta) w^3/\mu D)$, which can also be interpreted as a Rayleigh number. Note that $\lambda^*$ does not change systematically over more than two decades of Pe. The only experimental parameter that affected $\lambda^*$ substantially was $\theta$, for which $\lambda^* \sim 1/\sqrt{\cos(\theta)}$ (Fig. 2, right). For horizontal propagation the interface was smooth, verifying that the instability is driven by buoyancy.

These results contrast markedly to the scalings of Eq. 3, where for a given composition (fixed $\rho$, $\delta$, $\Sigma$, $\nu$, D), $\lambda^* \sim w^2/\cos(\theta)$. Moreover, Eq. 3 predicts $\lambda^*/w = (8\pi/3)Pe$, which is lower than observed values by factors of 30 to 1500. This indicates that some process other than diffusion suppresses high-k modes. In contrast, our results are entirely consistent with the scalings of Eq. (2), *i.e.* $\lambda^* \sim w^0/\sqrt{\cos(\theta)}$, suggesting that high-k modes are suppressed by surface tension – even though the reactants and products are miscible in all proportions. For a typical $\lambda^* = 10$ mm, $\delta = 6 \times 10^{-4}$ and $\theta = 0$, Eq. (2) predicts $\Sigma \approx 5 \times 10^{-3}$ dyne/cm, which is $1.4 \times 10^4$ times smaller than that between water and air at 22°C. Thus, a rather weak surface tension could cause the observed behavior.

Cahn and Hilliard [13] and Davis [14] suggest that for interfaces between miscible regular solutions having different solute concentrations

$$\Sigma = \int_{-\infty}^{\infty} \kappa \left( \frac{dC}{dx} \right)^2 dx \approx \kappa \frac{(\Delta C)^2}{\tau} \qquad (4),$$

where $\kappa$ is a constant, C is the local solute concentration and $\Delta C$ is the total concentration change across the interface. (Surface tension could also result from the thermal gradients caused by heat release, but the thermal diffusivity $\alpha >> D$ for most liquids, consequently the thermal $\tau$ is much

larger than the compositional $\tau$, and thus would result in a much lower induced $\Sigma$.) For reasons not yet clear to us, our results and those of other investigations for both reaction-diffusion fronts and displacement fronts are considerably better described by neglecting the $\Delta C$ effect and presuming $\Sigma \approx K/\tau$, consequently we will employ this relation instead.

For the aforementioned $\Sigma \approx 5 \times 10^{-3}$ dyne/cm and a typical s = 0.02 cm/s, we infer $K \approx \Sigma D/s = 3.5 \times 10^{-6}$ dyne. To determine a best-fit K for all our data, the effects of heat loss to the cell walls must be considered as follows. It is readily shown that the total thermal energy (thus thermally buoyant fluid) in the system is proportional to the ratio (H) of the heat generation rate ($=s^2/\alpha$) to heat loss rate ($=\alpha/w^2$), thus $H = (sw/\alpha)^2$. We expect that for $H << 1$, the thermal contribution to $\delta$ is lost via heat transfer to the walls, thus $\delta \approx \delta_C$, whereas for $H >> 1$, both thermal and compositional contributions are important, thus $\delta \approx \delta_C + \delta_T$. This requires $\lambda^*$(experiment)/ $\lambda^*$(theory, $\delta_C+\delta_T$) be larger than unity (corresponding to an overestimate of $\delta$) for small H, but decrease to unity at large H, and that $\lambda^*$(experiment)/ $\lambda^*$(theory, $\delta_C$) be close to unity at small H, but decrease to less than unity for large H. A best fit of our data to these requirements suggests $K \approx 2.0 \times 10^{-6}$ dyne (Fig. 3).

**Results - displacement fronts**

Shortly after removing the barrier strip, the fronts started to exhibit fingers, a typical image of which is shown in Fig. 1 (lower). Figure 4 shows that $\lambda^*/w$ was nearly constant ($\approx 10$) for a wide range of $\delta$, w and $\theta$ and different solutes, unlike reaction-diffusion fronts where $\lambda^*$ itself was nearly constant for $\theta = 0$. The prediction based on the diffusion model (Eq. 3) is $\lambda^*/w = 8\pi/(3(\sqrt{5}-2)Pe)$, which is far smaller than experimental values except at very small Pe, thus we again consult the surface tension model. For non-reacting interfaces, the model must be modified since $\tau$ and thus $\Sigma$ is not prescribed *a priori* by the balance between chemical reaction and diffusion. Since diffusion thickens the front while buoyant convection thins it, we estimate $\tau$ as D/U where again $U = \sigma^*/k^*$, and thus $\Sigma^* = K\sigma^*/Dk^*$. Equation (1) then leads to

$$\lambda^* = \pi w\sqrt{\frac{K}{3\mu D}};\ \ \sigma^* = \frac{\rho g\delta\cos(\theta)w}{18}\sqrt{\frac{3D}{K\mu}};\ \ \Sigma^* = \frac{\rho g\delta\cos(\theta)w^2K}{36\mu D} \qquad (5)$$

For our conditions ($\mu$ = 0.010 g/cm-s and D = 6.0 x $10^{-6}$ $cm^2/s$ for $KMnO_4$ [2]), *using K = 2.0 x $10^{-6}$ dyne as for reaction-diffusion fronts*, Eq. 5 predicts $\lambda^*/w = 10.4$. For Pe > 50, this is close to our measured values (Fig. 4) for a two-decade range of Pe, as well as a data point from Wooding [2], who mainly examined the nonlinear growth of large amplitude fingers but for two cases ($\theta$ = 34.1°, 87.1°) reported an initial $\lambda^*$.

Our apparatus did not permit low enough Pe to examine diffusion-*dominated* fingering, which should result in $\lambda^*/w$ given by Eq. 3, but a transition to diffusion-*affected* behavior is seen in Fig. 4 at Pe < 50. Our data are consistent with Wooding's data point in this regime. The transition is expected when values of $\sigma^*$ from Eqs. 3 and 5 are equal, which corresponds to Pe = $\sqrt{\mu D/108C_2^2K} \approx 43$ for our conditions, which is close to the observed transition. The Pe << 1 regime has recently been studied extensively [15] and good agreement with Eq. 3 is found.

**Comparison to prior works**

Carey *et al.* [5] studied rising reacting-diffusion fronts with very small s (0.00035 cm/s) and $\delta$ (4.0 x $10^{-5}$) in Hele-Shaw cells with $0.40 \le w \le 0.94$ mm. They claim that their measured $\lambda^*$ are consistent the diffusion model (Eq. 3), however, their Fig. 2 shows that for w > 0.5 mm, the data are fit equally well by a constant $\lambda^* \approx 5$ mm, which is consistent with the surface tension model. Using Eq. 2 for their test conditions then implies $\Sigma \approx 8.3 \times 10^{-5}$ dyne/cm and K = 3.3 x $10^{-6}$ dyne. The transition from diffusion to surface tension controlled behavior should occur when $\sigma^*$ from Eqs. 2 and 3 are equal. This corresponds to Pe = $(1024/27)(\mu D^2/wKs)$ or w = 0.54 mm for their conditions, which is close to their apparent transition from $\lambda^* \sim w^{-2}$ to $\lambda^* \sim w^0$.

Mayer and collaborators [16] measured an apparent $\Sigma$ at dissolving isobutyric acid/water (IBW) and cyclohexane/methanol (CM) interfaces using a capillary-wave technique. $\Sigma$ varied as $1/\sqrt{Dt} \sim 1/\tau$, where t is the time lapse since the mixture was heated from a two-phase

(immiscible) to a one-phase (miscible) equilibrium condition, which is consistent with the relation $\Sigma = K/\tau$. For IBW at t = 5700 s, with a measured $\Sigma = 1.6 \times 10^{-4}$ dyne/cm and a reported $D = 1.8 \times 10^{-8}$ cm$^2$/s, we infer $K = 1.6 \times 10^{-6}$ dyne. For CW at $t = 2 \times 10^4$ s, $\Sigma = 8 \times 10^{-5}$ dyne/cm and $D = 1.4 \times 10^{-8}$ cm$^2$/s, we infer $K = 4.2 \times 10^{-6}$ dyne.

Matthiessen *et al.* [17] showed that for thin (≈ 1mm) horizontal layers of Belousov-Zhabotinskii reactants, the surface tension gradient at the free surface due to compositional changes across the front dominated buoyancy as a flow driving mechanism. They did not explicitly determine Σ, but found that the measured and calculated convection velocity profiles were best fit by a solutal Marangoni number of 0.3. While the Σ gradient at the free surface is not directly related to Σ across the chemical interface in the bulk fluid discussed in this work, their Marangoni number can be used to infer $d\Sigma/dx \approx 0.0194$ dyne/cm$^2$. Using their presumed $\tau \approx 0.018$ cm, an apparent $K \approx 6.3 \times 10^{-6}$ dyne can be inferred.

Patterson [18] examined fingering in miscible fronts of water displacing glycerin in horizontal Hele-Shaw cells, where the viscosity contrast rather than buoyancy drives the instability. With $\mu_1 >> \mu_2$, g = 0 and $\Sigma = KU/D$, where in this case U is a forced displacement speed, Eq. 1 predicts $\lambda^* / w = \pi\sqrt{K/\mu_1 D}$. With Patterson's measured $\lambda^*/w = 4$, $\mu_1 = 10.2$ g/cm-s and $D = 1.7 \times 10^{-7}$ cm$^2$/s [8], we infer $K \approx 2.8 \times 10^{-6}$ dyne.

**Discussion**

Our results show that interfaces between miscible fluids possess a weak surface tension that affects the interfacial stability and resulting flow, typically more significantly than diffusion. An empirical constant $K = \Sigma\tau \approx 4 \pm 2 \times 10^{-6}$ dyne describes a broad range of experimental results. This magnitude of K might be anticipated since the maximum attractive force between water molecules based on the Stockmayer potential is $(504/169)(7/26)^{1/6}(5.2 \times 10^{-14}$ erg$)/(2.6 \times 10^{-8}$ cm$) = 4.8 \times 10^{-6}$ dyne. Davis [14] recommended $K = 2 \times 10^{-6}$ dyne for hydrocarbons but gave no justification. While we have not determined the limits of applicability of our K value,

even for an immiscible water-air interface with $\tau \approx 10^{-7}$ cm, the prediction $\Sigma \approx 40$ dyne/cm has the right order of magnitude.

We thank Drs. H. T. Davis, S. Davis, J. Goddard, T. Maxworthy and P. Petitjeans for helpful discussions. This work was supported by NASA grants NAG3-1523 and NAG3-2124.

**References**

1. G. M. Homsy, *Ann. Rev. Fluid Mech.* **19**, 271, 1987.
2. R. A. Wooding, *J. Fluid Mech.* **39**, 477 (1969).
3. J. Huang, D. A. Vasquez, B. F. Edwards, P. Kolodner, *Phys. Rev. E* **48**, 4378 (1993); J. Huang, B. F. Edwards, *Phys. Rev. E* **54**, 2620 (1996).
4. D. A. Vasquez, J. W. Wilder, B. F. Edwards, *J. Chem. Phys.* **104**, 9926 (1996); J.-Y. Zhu, *Phys. Fluids* **10**, 775 (1998).
5. M. R. Carey, S. W. Morris, P. Kolodner, *Phys. Rev. E* **53**, 6012 (1996).
6. P. G. Saffman, G. I. Taylor, *Proc. Roy. Soc. (London)* **245**, 312 (1958).
7. Gardner, J. W., Ypma, J. G. J., *SPE 10686*, Soc. Pet. Eng., Dallas, TX (1982).
8. P. Petitjeans, T. Maxworthy, *J. Fluid. Mech.* **326**, 37 (1996).
9. P. Petitjeans, *C. R. Acad. Sci. Paris. serie IIb* 322, **673** (1996) (in French).
10. A summary of earlier investigations is given by D. D. Joseph, Y. Y. Renardy, in: *Fundamentals of Two-Fluid Dynamics. Part II: Lubricated transport, drops and miscible liquids*, Chapter X, Springer-Verlag, New York (1993).
11. L. Szirovicza, I. Nagypal, E. Boga, *J. Am. Chem. Soc.* **111**, 2842 (1989).
12. A. Hanna, A. Saul, K. Showalter, *J. Am. Chem. Soc.* **104**, 3838 (1982).
13. J. W. Cahn, J. E Hilliard, *J. Chem. Phys.* **28**, 258 (1958).
14. H. T. Davis, in: *Numerical Simulation in Oil Recovery* (M. Wheeler, Ed.), Springer-Verlag, p. 105 (1988).
15. J. Fernandez, P. Kurowski, P. Petitjeans (to be published).
16. May, S. E., Maher, J. V., *Phys. Rev. Lett.* **67**, 2013 (1991); Vlad, D. H., Maher, J. V., *Phys. Rev. E.* **59**, 476 (1999).
17. K. Matthiessen, H. Wilke, S. C. Müller, *Phys. Rev. E* **53**, 6056 (1996).
18. Patterson, L., *Phys. Fluids.* **28**, 26 (1984).

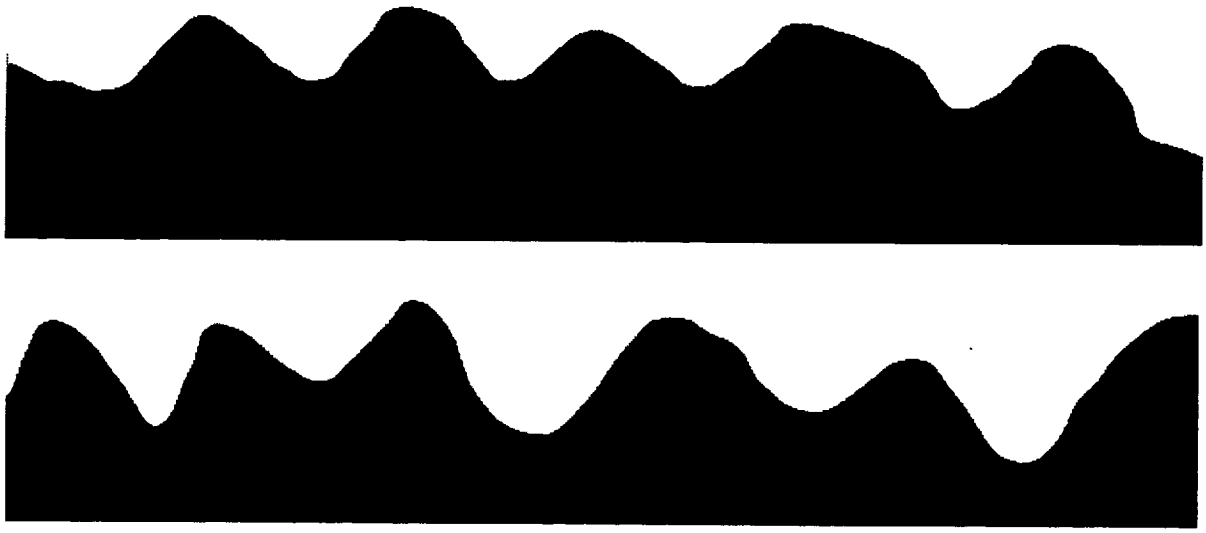

Figure 1. Contrast-enhanced images of interfaces in Hele-Shaw cells. Upper: upward propagating reaction-diffusion front with s = 0.0038 cm/s, w = 1.0 mm, $\delta$ = 0.00032, Pe = 63, field of view 5.0 cm wide. Lower: non-reacting displacement front of water over water/ethanol solution with $KMnO_4$ dye, w = 0.80 mm, $\delta$ = -0.00036, $\theta$ = 180°, Pe = 85, field of view 5.4 cm wide.

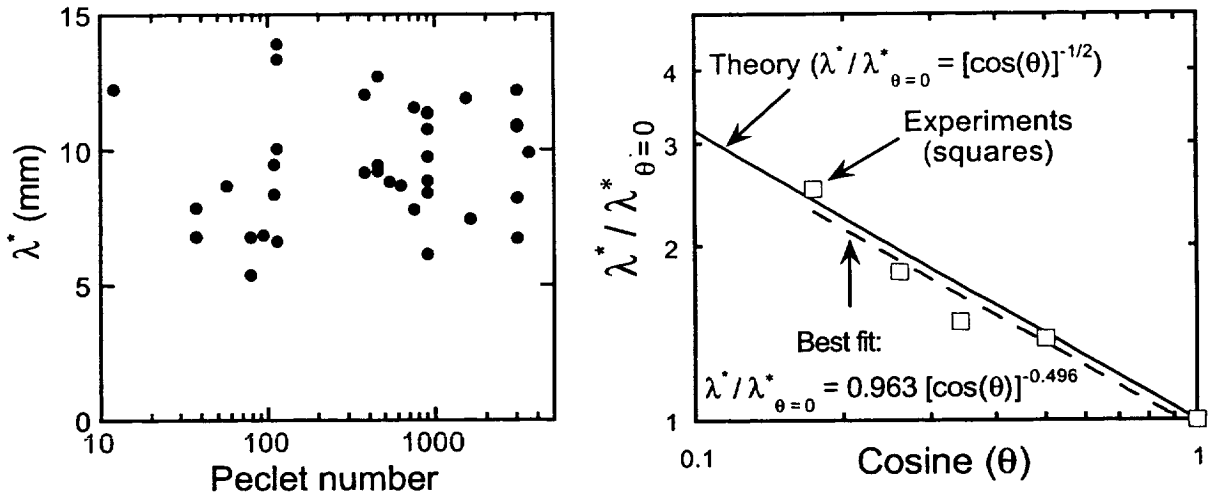


Figure 2. Observed instability wavelengths ($\lambda^*$) for upward propagating reaction-diffusion fronts in Hele-Shaw cells. Left: as a function of the Peclet number = $(1/36)(\rho g \delta \cos(\theta) w^3/\mu D)$, for vertical cell orientation ($\theta = 0$). Mean and standard deviation for all points shown are 9.5 mm and 2.2 mm, respectively. Right: as a function of $\theta$ for s = 0.02 cm/s and w = 1.0 mm.

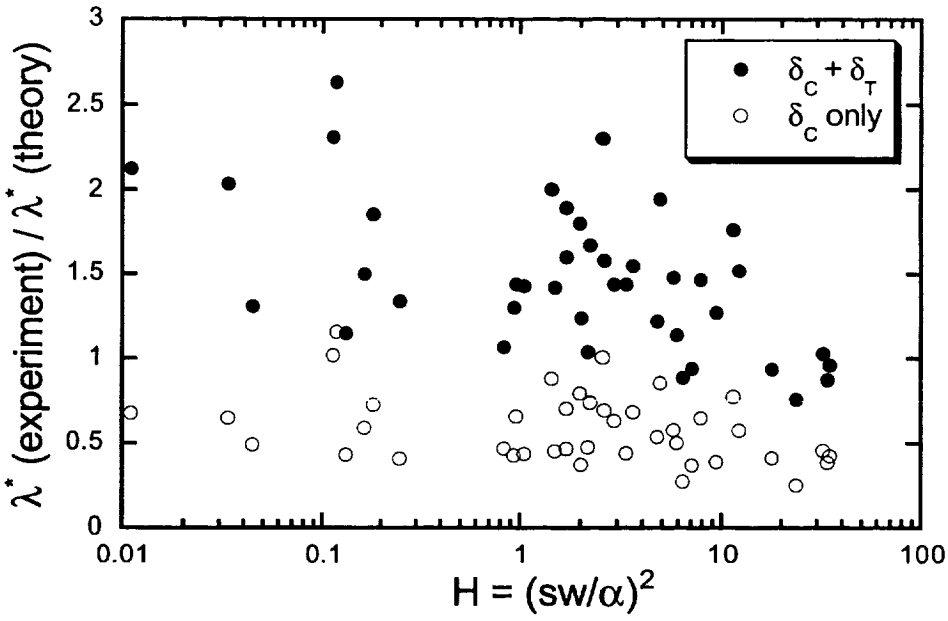


Figure 3. Comparison of measured and predicted (Eq. 2, using $\Sigma = Ks/D$, with $K = 2 \times 10^{-6}$ dyne) instability wavelengths for dimensionless density contrasts due to both thermal and composition changes ($\delta_T + \delta_C$) and composition changes ($\delta_C$) only, as a function of the heat loss parameter H.

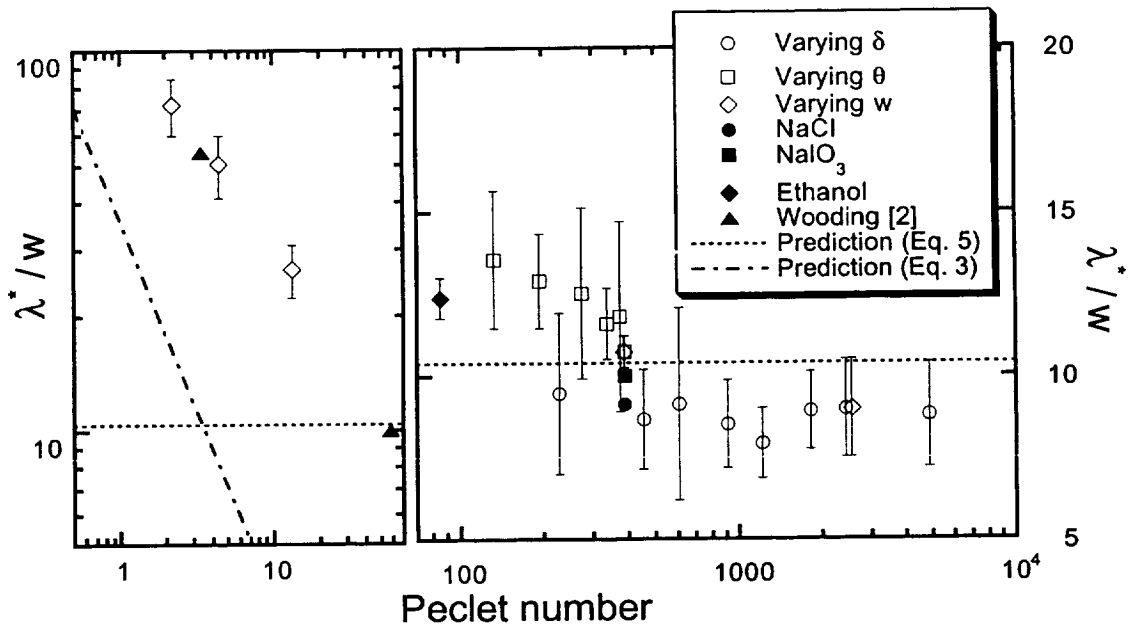


Figure 4. Measured initial instability wavelengths ($\lambda^*$), referenced to the cell thickness (w), for non-reacting solute-water solutions over or under water, as a function of the Peclet number, along with the predictions of Eqs. 3 and 5 for $K = 2 \times 10^{-6}$ dyne. For the data set of varying $\delta$, the solute is $KMnO_4$, w = 1.3 mm and $\theta = 0$. For the data set of varying $\theta$, $\delta$, the solute is $KMnO_4$, w = 0.80 mm and $\delta = 0.0017$. For the NaCl and $NaIO_3$ data points, w = 0.80 mm, $\delta = 0.0017$ and $\theta = 0$. For the ethanol data point, w = 0.80 mm, $\delta = -0.00036$ and $\theta = 180°$. Where shown, error bars correspond to one standard deviation of the measured $\lambda^*$ for one test.